Journal of Experimental Botany Advance Access published November 4, 2014

Journal of Experimental Botany
doi:10.1093/jxb/eru409

Journal of Experimental Botany
www.jxb.oxfordjournals.org

RESEARCH PAPER

SASP, a Senescence-Associated Subtilisin Protease, is involved in reproductive development and determination of silique number in *Arabidopsis*

Dana E. Martinez[1,*], Maria L. Borniego[1], Natalia Battchikova[2], Eva-Mari Aro[2], Esa Tyystjärvi[2] and Juan J. Guiamét[1]

[1] Instituto de Fisiología Vegetal (INFIVE) – Consejo Nacional de Investigaciones Científicas y Técnicas (CONICET), Universidad Nacional de La Plata, Argentina
[2] Molecular Plant Biology, Department of Biochemistry, University of Turku, FI-20014 Turku, Finland

* To whom correspondence should be addressed. E-mail: danamartinez@conicet.gov.ar

Received 21 July 2014; Revised 3 September 2014; Accepted 8 September 2014

Abstract

Senescence involves increased expression of proteases, which may participate in nitrogen recycling or cellular signalling. 2D zymograms detected two protein species with increased proteolytic activity in senescing leaves of *Arabidopsis thaliana*. A proteomic analysis revealed that both protein species correspond to a subtilisin protease encoded by At3g14067, termed Senescence-Associated Subtilisin Protease (SASP). *SASP* mRNA levels and enzyme activity increase during leaf senescence in leaves senescing during both the vegetative or the reproductive phase of the plant life cycle, but this increase is more pronounced in reproductive plants. *SASP* is expressed in all above-ground organs, but not in roots. Putative AtSASP orthologues were identified in dicot and monocot crop species. A phylogenetic analysis shows AtSASP and its putative orthologues clustering in one discrete group of subtilisin proteases in which no other *Arabidospsis* subtilisin protease is present. Phenotypic analysis of two knockout lines for *SASP* showed that mutant plants develop more inflorescence branches during reproductive development. Both *AtSASP* and its putative rice orthologue (*OsSASP*) were constitutively expressed in *sasp-1* to complement the mutant phenotype. At maturity, *sasp-1* plants produced 25% more inflorescence branches and siliques than either the wild-type or the rescued lines. These differences were mostly due to an increased number of second and third order branches. The increased number of siliques was compensated for by a small decrease (5.0%) in seed size. *SASP* downregulates branching and silique production during monocarpic senescence, and its function is at least partially conserved between *Arabidopsis* and rice.

Key words: At3g14067, inflorescence, protease activity, reproductive development, senescence, subtilisin protease.

Introduction

Senescence is the final stage of the development of plant organs, or of the whole plant in monocarpic species (Noodén *et al*, 2004). It is functionally characterized as a highly organized and regulated stage of massive degradation of macromolecules, with a concomitant release of nutrients. The reallocation of nutrients released from senescing organs, particularly nitrogen from proteins, supports the development of younger leaves or seeds, and thus senescence functions as a salvage mechanism that dramatically impacts crop yield (Chardon *et al.*, 2012; Gregersen *et al.*, 2013).

Proteases play a critical role in senescence as catalysts of bulk protein degradation, but also as enzymes of the regulatory network underlying catabolic pathways (Beers at al., 2003; Rojo *et al.*, 2003). Strikingly, understanding of the

Abbreviations: SBT, subtilisin protease; SASP, senescence-associated subtilisin protease; AtSASP, *Arabidopsis* SASP; OsSASP, rice SASP.

proteolytic mechanism responsible for the massive degradation of Rubisco and other plastid proteins, a hallmark of leaf senescence, remains incomplete. Many proteases are upregulated or specifically expressed during leaf senescence (Buchanan-Wollaston *et al.*, 2003, Guo *et al.*, 2004). These proteases localize to different organelles and cell compartments, and display different temporal expression profiles and responses to hormones or stress treatments that alter the onset or rate of senescence (Otegui *et al.*, 2005; Parrot *et al.*, 2010; reviewed in Roberts *et al.*, 2011) which suggests a high degree of specificity and/or non-redundancy for some proteolytic functions. For instance, an aleurain-like cysteine protease (cys-protease) from Broccoli, BoCP5, is expressed during leaf and flower senescence, and transgenic broccoli plants with downregulated BoCP5 show delayed postharvest floret senescence (Eason *et al.*, 2005). Plant metalloproteases are involved in extracellular processes during senescence and cell death (Delorme *et al.*, 2000; Martínez and Guiamet, 2014). The matrix metalloproteinase At2-MMP is expressed in most organs, with strong induction after the plant enters the reproductive phase and senesces. Mutant *at2-mmp* plants show less growth, late flowering, and early senescence (Golldack *et al.*, 2002).The chloroplast-located aspartic protease (Asp-protease) CND41 shows chloroplast DNA-binding capacity (Nakano *et al.*, 1997) and degrades partially denatured Rubisco *in vitro* (Kato *et al.*, 2004). CND41 antisense tobacco lines show retarded leaf senescence (Kato *et al.*, 2004), whereas tobacco lines overexpressing CND41 show enhanced leaf senescence, specifically in the lower leaves of plants during the reproductive phase (Kato *et al.*, 2005). NANA is the closest homologue to CND41 in *Arabidopsis*, and *nana* mutants display dwarfism, small leaves, and delayed flowering. NANA mis-expression affects photoassimilate partitioning and starch turnover, limiting metabolism and growth (Paparelli *et al.*, 2012). CND41/NANA, At2-*MMP*, and BoCP5, as well as other proteases, might affect senescence by exerting an indirect effect on plant growth. Leaf senescence is also controlled by correlative effects from younger and growing parts of the plant (i.e. the developing shoot apex; Noodén *et al.* 2004). Hence, it is not surprising that manipulation of leaf senescence-associated proteases may have a direct impact on plant growth and development.

Functional analyses of previously identified senescence-associated proteases are scarce. Posttranslational modifications might represent key regulatory steps for constitutively expressed proteases involved in senescence, making their identification more challenging (Rojo *et al.*, 2003; Gu *et al.*, 2012). For instance, saspases, which are a type of plant subtilisin-like serine proteases, are constitutively present in their active form inside the cell, but are shifted to the extracellular fluid upon induction of programmed cell death by a fungal toxin (Coffeen and Wolpert, 2004, Vartapetian *et al.*, 2011).

Activity-based protease detection (ABPD) is a straightforward approach for the study of senescence-related proteases. Zymography is a versatile ABPD technique that allows for the simultaneous detection of a variety of hydrolytic activities based on the protease molecular weight, and/or isoelectric point, with nanoscale sensitivity (Chung *et al.*, 2011; Vandooren *et al.*, 2013). The technique is based on the use of polyacrylamide gels co-polymerized with a non-specific substrate for proteases (gelatin and casein); once the electrophoresis run is complete, the gel is incubated under specific conditions (pH, reagents, and incubation time) to promote protease activity, which becomes evident after gel staining as clear bands against a stained background. Zymography has allowed the detection and characterization of many senescence-related proteases (Wagstaff *et al.*, 2002; Martinez *et al.*, 2007; Rossano *et al.*, 2011; Grudkowska *et al.*, 2013).

In the present study, zymography was combined with proteomic techniques to detect and identify proteases with activities associated with leaf senescence. The subtilisin type (SBT) serine protease SBT1.4/*AtSASP* from *Arabidopsis* was detected and then identified with this methodology. To further investigate the specific role of the detected senescence-associated protease, loss-of-function and gain-of-function mutants were analysed, showing that SBT1.4/*AtSASP* affects reproductive development and yield. Complementation of *at-sasp* plants with the rice homologue Os*SASP* gives insight into a potential conserved function of SASP proteases in *Arabidopsis* and rice.

Materials and methods

Plant materials

Arabidopsis thaliana SALK lines (ecotype Columbia Col-0) with T-DNA insertions in *SASP* (At3g14067) were selected using the SIGnAl database and obtained from ABRC (www.abrc.osu.edu). Homozygous knockout plants for *SASP* (*sasp-1*, SALK_147962; *sasp-2*, SALK_063823) were identified by PCR using the SALK T-DNA Primer Design Program (http://signal.salk.edu/tdnaprimers.2.html; see Supplementary Table S3). Homozygous plants for the T-DNA insertion were analysed for SASP activity in zymograms. *Oryza sativa* L. japonica cv. Nipponbare was used as a model rice plant.

Plant growth conditions, sampling, and harvest

Arabidopsis plants were cultivated in growth chambers, in pots (9 cm diameter × 13 cm depth) filled with soil and vermiculite at a ratio of 3:1 (v/v), with one plant per pot, at 20°C and 90 or 150 µmol m^{-2} s^{-1} photosynthetic photon flux density (PPFD) provided by tungsten-halogen or fluorescent lamps. Plants were grown under an 8 h light/16 h dark photoperiod for the first 2 weeks, and under a 16 h light/8 h dark photoperiod thereafter. Rice was grown in a greenhouse with controlled temperature and humidity.

Leaf chlorophyll content

Chlorophyll was measured with the SPAD 502 Portable Chlorophyll Meter (Minolta®).

Protein extraction

For 1D SDS-PAGE gels and zymograms, leaves were homogenized in 50 mM Tris pH 7.5, 20 mM cysteine, and 1.0% insoluble polyvinylpyrrolidone, and centrifuged at 12 000*g*, 4°C for 15 min. Sample buffer (Laemmli, 1970) was added before electrophoresis. For 2D gels, leaf extracts were solubilized in 25 mM Tris pH 7.5, 20 mM cysteine and passed through a 10 kD cut-off desalting column (Microcon®, Millipore). Proteins were recovered in 250 µl water, 2.0% Triton X-100, 15 mM DTT, 2M urea, 20 µm leupeptin, and

0.2% ampholytes (pH 4–7, Bio-Rad), and cleared by centrifugation at 90 000*g* for 20 min at 4°C.

1D and 2D (isoelectric focusing SDS-PAGE) electrophoresis

Isoelectric focusing (IEF) was performed in immobilized pH gradient strips (IPG) in a pH range of 3–10 in a BioRad IEF Cell using the following program: 50 V-4h, 100 V-1h, 200 V-1h, and 10 000 V until 60 000 Vh. The strips were equilibrated in Laemmli buffer before running in the second dimension (SDS-PAGE). SDS-PAGE gels (1D and 2D) were made of 12% w/v acrylamide with or without 0.04% w/v gelatin and run at 4°C. Activity gels were stained with Coomassie-Brillant Blue (CBB) whereas conventional gels (without gelatin) were CBB or silver stained (Shevchenko *et al.*, 1996).

Zymography

Activity gels (1D or 2D SDS-PAGE gels containing 0.04% w/v gelatin) were washed after electrophoresis in 80 mM AcNa pH 5.0, 2.0% Triton X-100 for at least 1 h and incubated in 80 mM AcNa pH 5.0, 20 mM DTT at 37°C overnight. Proteolytic activity developed as white bands or spots (1D or 2D gels, respectively) in a CBB background. The proteases responsible for senescence-associated proteolytic activity were detected in the silver-stained gel by superimposing 2D silver-stained and 2D activity gels.

Immunodetection

Leaves were homogenized in 50 mM Tris pH 8.0, 20 mM cysteine, 1.0% insoluble polyvinylpyrrolydone, 10% glycerol, 50 mM phenylmethylsulfonylfluoride, and 2 mM 4-(2-aminoethyl)-benzenesulfonyl fluoride hydrochloride. Samples were centrifuged at 12 000*g* for 15 min and loaded immediately in pre-cooled 12% w/v acrylamide SDS-PAGE gels. After electrophoresis, proteins were electrotransferred to a nitrocellulose membrane. All the steps were performed at 4°C. The membrane was blocked with 10% non-fat milk, and incubated with a monoclonal anti-GFP antibody (Roche®); Anti-Horseradish Peroxidase was used as secondary antibody.

Mass spectrometry analysis and protein identification

The spots corresponding to the proteases of interest were excised from the silver-stained gel, destained, dried, reduced, alkylated, and Trypsin digested (Trypsin Gold, Promega). The resulting peptides were washed with 5% formic acid and 80% acetonitrile, concentrated, and desalted following Zhang *et al.* (2004). Samples were analysed in an LC-ESI MS/MS (API QSTAR) Nano Electrospray Protana (Applied Biosystems, Toronto). Protein identification was performed with the Mascot search engine (MatrixScience, http://www.matrixscience.com) using the National Center for Biotechnology Information non-redundant database. Errors < 100 ppm were omitted.

RNA extraction and gene expression analysis

Total RNA was isolated from 100 mg leaves following Sanchez and Carbajosa (2008). Reverse transcription was performed at 25°C for 10 min, 42°C for 2 h, and 70°C for 15 min using reverse transcriptase (Fermentas) and random primers (1 mM; Invitrogen). Primers used for RT-PCR amplification of AtSASP, OsSASP, YFP, and Actin2 (amplified as a loading control) are listed in Supplementary Table S3.

For quantitative RT-PCR (qRT-PCR), total RNA was isolated using the RNeasy Plant Mini Kit (Qiagen). RT-PCR was performed at 25°C for 10 min, 37°C for 1 h, and 72°C for 5 min from 100 ng of total RNA using M-MLV reverse transcriptase (Promega, Madison, WI, USA) and random primers (1 mM; Invitrogen). qPCR was performed in an iCycler real-time PCR (Bio-Rad, Munich,Germany) using SybrGreen mix (Invitrogen). AtSASP primers 12 and 13 were designed with the Chromas Primer Designer program to amplify a fragment of 614 bp from the subtilisin transcript. The running protocol was as follows: cycle 1 (×1) 95°C 10 min; cycle 2 (×50) 95°C 15 s, 57°C 15 s, and 72°C 30 s; and cycle 3 (×81) 55–95°C 30 s. The comparative Ct method was used to quantify AtSASP transcript and normalization was performed with the UBQ10 housekeeping gene. Values are expressed as the average ± SD. Representative experiments were performed three times and analysed statistically using the Mann–Whitney *U*-test.

Subcloning of AtSASP *and* OsSASP *and complementation of* sasp-1 *plants*

The binary vector pCAMYFP was generated by cloning the 35S-EYFP-nos cassette from the pAN vector (Nelson *et al.*, 2007, http://www.bio.utk.edu/cellbiol/markers/) into pCAMBIA 1300. AtSASP (At3g14067) and OsSASP (Os02g779200) gene coding regions were PCR amplified from genomic DNA using Phusion taq polymerase (Fermentas) with the primers 6–7 and 8–9 for AtSASP and OsSASP, respectively (Supplementary Table S3). The primers were engineered with SpeI and XbaI restriction sites (Supplementary Table S3). The PCR products were sequenced, SpeI and XbaI or XbaI digested, and cloned into pCAMYFP to form pCAM35S:AtSASP:YFP and pCAM35S:OsSASP:YFP, respectively. The constructions were sequenced from the 35S and YFP flanking regions (primers 10 and 11), and transferred into *Agrobacterium tumefaciens* (strain GV3101) using the freeze-thaw method (Wise *et al.*, 2006). *Agrobacterium* was then used to transform homozygous *sasp-1* plants by floral dip (Clough and Bent, 1998). Seeds obtained from the transformed plants (AtSASP:YFP-*sasp1* and OsSASP:YFP-*sasp1* plants) were selected on plates containing 15 mg l^{-1} hygromycin, and the presence of the construct was confirmed by PCR with the primers used for genomic AtSASP and OsSASP amplification.

Sequence alignment and phylogenetic analysis

As a first step, SASP was compared to other *Arabidopsis* subtilisin proteases by performing a BLASTP search in the *Arabidopsis* genome (http://www.arabidopsis.org/Blast/index.jsp). The 10 proteins showing the highest sequence similarity to SASP were examined for expression by eFP Browser Database analysis. (Winter *et al.*, 2007) (Supplementary Table S1).

As a second step, SASP amino acid sequence was used as query sequence for a BLASTP search at NCBI against non-redundant protein sequences (non-redundant GenBank CDS translations), BLASTP 2.2.27. The best hits excluding sequences from *Arabidopsis* (Supplementary Table S2) were selected for further multiple sequence alignment.

Protein sequences retrieved from both the TAIR and NCBI BLASTP were combined in a multiple alignment using COBALT RID. The tree was obtained by the neighbour-joining approach with COBALT software, with the default parameter setting, Grishin Distance, 0.85 Max Seq Difference (http://www.ncbi.nlm.nih.gov/tools/cobalt/ with default settings) (Papadopoulos and Agarwala, 2007), (Supplementary Figure S2).

Statistical analysis

Results shown correspond to one experiment representative of an average of several independent experimental sets, and values are the mean and SE of a pool of at least eight plants. Means were compared with the Student's *t*-test ($P < 0.05$). Statistical significance was determined with a one-way analysis of variance using STATISTICA Software, and the LSD test ($P < 0.05$).

Accession numbers

Sequence data for SASP can be found in the GenBank/EMBL data libraries under the accession number At3g14067. Accession numbers to GenBank/EMBL corresponding to other sequences can be found in Supplementary Tables 1 and 2.

Results

Detection of leaf senescence-associated proteolytic activity and identification of AtSASP as one of the responsible proteases

To identify proteases whose activity increases or is specific to senescing leaves, we compared the active protease profiles from young, mature, and early- and late-senescing leaves. Senescence stages were defined based on the protein and chlorophyll contents in a given leaf area, considering early and late senescence as a drop of 30–50 and 70% of the protein and chlorophyll contents, respectively, compared to those at the mature stage (Table 1). Leaf soluble protein extracts were run in parallel in SDS-PAGE and in activity SDS-PAGE gels (zymograms). The zymogram revealed bands of proteolytic activity that decreased, increased, or remained constant during the time course of leaf senescence (Fig. 1A). One active band with a molecular weight slightly higher than that of the Rubisco large subunit became more intense during early and late senescence (Fig. 1A: box in the zymogram). With a better resolution, achieved by mild variations in the amount of sample loaded onto the gel and in the zymogram development time, the senescence-associated activity could be resolved into two bands, with apparent molecular masses of 59 and 61 kD (Fig. 1B, left gel). To separate the proteases responsible for the two activity bands, protein extracts from senescing leaves were run simultaneously in preparative 2D IEF/SDS-PAGE gels and 2D zymograms (Fig. 1B). 2D zymograms resolved the senescence-related protease activity bands as two spots with slightly different isoelectric points (Fig. 1B, middle gel) which were also detected in the silver-stained 2D gel (Fig. 1B, right gel). Activity and silver-stained spots show a perfect match when 2D gels and 2D zymograms are aligned. The two spots corresponding to the active proteases were excised from the silver-stained gel and subjected to mass fingerprinting analysis. Both spots were identified as corresponding to the subtilisin-like serine protease, subtilase AtSBT1.4, encoded by the locus At3g14067 (Fig. 1C). Due to its increased activity during senescence, we named SBT1.4 as Senescence Associated Subtilisin Protease (SASP). The AtSBT1.4/AtSASP protein has a nominal molecular mass of 81.8 kD (http://www.uniprot.org), corresponding to the pre-pro-protease precursor, whereas the experimental masses calculated from zymograms are 59 and 61 kD, in the size range of mature forms of subtilisin proteases (Berger and Altmann, 2000; Beers *et al.*, 2003). The occurrence of the two variant forms of AtSASP could be due to posttranslational modifications. The identification of At3g14067 in a proteomic analysis of secreted glycoproteins (Table 2 in Minic *et al.*, 2007) supports this possibility.

Table 1. *Percentage of leaf chlorophyll and soluble protein content in young leaves and early- and late-senescing leaves, with respect to mature leaves, quantified on a leaf area basis*[a]

	Y	M	S_1	S_2
Protein (%)	94	100	76	30
Chlorophyll (%)	78	100	50	30

[a] Y, young leaves; M, mature leaves; S_1, early-senescing leaves; S_2, late-senescing leaves.

AtSASP expression and proteolytic activity are upregulated during leaf senescence in an organ-specific and plant age-dependent manner

According to data from DNA m*icroarrays (eFP Browser* DNA *Database:* Winter *et al.*, 2007*) AtSASP* is highly upregulated in senescing leaves, and also, to a lesser extent, in cauline leaves of the main shoot (Supplementary Figure S1). This suggests

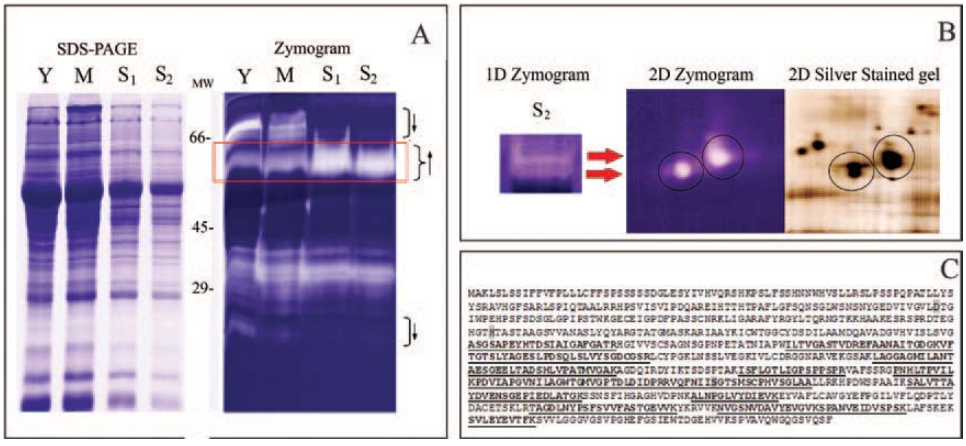

Fig. 1. Activity-based detection of leaf senescence-associated proteases and identification of AtSASP. (A) Time course analysis of protein content and proteolytic activity during leaf senescence shown using SDS-PAGE (left) and a zymogram (right), respectively Y, young leaves; M, mature leaves; S_1, early-senescing leaves; S_2, late-senescing leaves. Chlorophyll and soluble protein were compared on a leaf area basis (Table 1). Arrows indicate active proteases that increase or decrease during senescence. The box highlights proteolytic activity that becomes more intense in senescing leaves. (B) Purification of active proteases. Left: section of a 1D zymogram of S_2 leaves corresponding to the box in panel (A) showing two bands responsible for the senescence-associated proteolytic activity. Right: parts of 2D zymograms and 2D gels resolving the two activity bands as two spots of activity and silver-stained spots, respectively. (C) SBT4/AtSASP amino acid sequence. Ten peptide sequences were identified by mass spectrometry (in bold and underlined), with a 35% sequence coverage. Grey boxes depict the amino acid residues that constitute the catalytic tryad. This figure is available in colour at *JXB* online.

Table 2. *Total number of inflorescence branches and siliques produced per plant by the end of the life span, 10 weeks after flowering*[a]

Light conditions	No. of inflorescence branches per plant		No. of siliques per plant		Increase in *sasp-1* with respect to the wild type (%)	
	WT	*sasp-1*	WT	*sasp-1*	WT	*sasp-1*
90 µmol m^{-2} s^{-1}	41.2	52.2	42.4	47.9	26.7	13
150 µmol m^{-2} s^{-1}	33.4	48.2*	412.8	585.4*	45.5	42
% Difference, 90 vs 150 µmol m^{-2} s^{-1}	23.35	8.30	–2.71	18.18		

[a] Values represent the average of eight plants. Statistically significant differences between genotypes: *$P < 0.05$. WT, wild type.

that AtSASP proteolytic activity might be regulated at the transcriptional level, with *AtSASP* gene expression increasing at late stages of leaf and plant development. *Arabidopsis* undergoes whole plant (monocarpic) senescence triggered by the formation of reproductive organs (Nooden and Penney, 2001). To determine whether the transcriptional regulation of *AtSASP* in rosette leaves is organ autonomous or influenced by the whole plant developmental stage we performed a qRT-PCR analysis of the relative expression levels of *AtSASP* in senescing and non-senescing rosette leaves from plants at the vegetative and reproductive phases (14 d after flowering) (Fig. 2A). *AtSASP* gene expression was around 4-fold higher in senescing than non-senescing leaves, regardless of the plant developmental phase. Also, an increase in mRNA levels was observed when transcripts from reproductive plants were compared with those from plants at the vegetative phase, regardless of the leaf senescence stage. This suggests that *AtSASP* expression is also associated with reproduction and whole plant senescence, not just leaf senescence. The linkage between the increment of *AtSASP* transcript abundance (Fig. 2A) and proteolytic activity (Fig. 2B) suggests that AtSASP activity might increase due to a bigger pool of available protein. Zymography also revealed AtSASP activity in cauline leaves, inflorescence stems, branches and siliques, but not in roots (Supplementary Fig. S2).

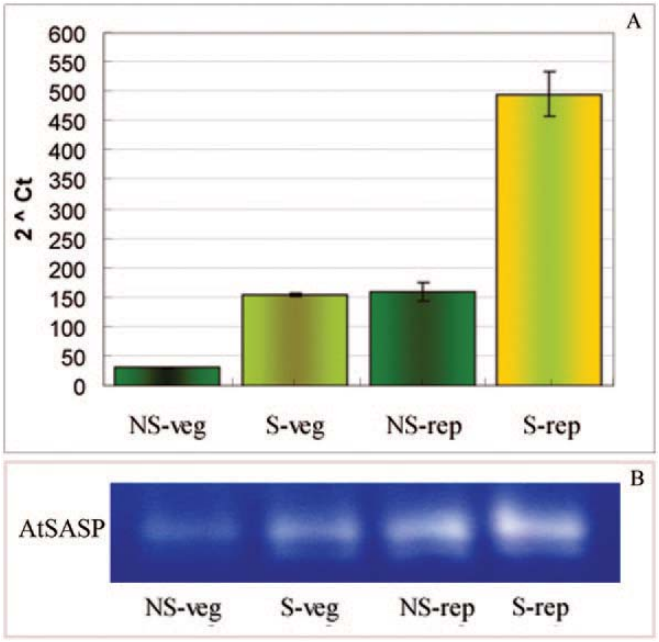

Fig. 2. Transcriptional regulation of *AtSASP*. (A) qRT-PCR analysis of the relative expression levels of *AtSASP* in leaves. NS-veg, non-senescing leaves at the vegetative stage; S-veg, senescing leaves at the vegetative stage; vegetative stage is 30 d after emergence (DAE). NS-rep, non-senescing leaves at reproductive stage; S-rep, senescing leaves at reproductive stage; reproductive stage is 60 DAE, 14 d after flowering. Relative levels are normalized to those of POLYUBIQUITIN 10 (*UBQ10*) transcripts. (B) AtSASP activity in NS-veg, S-veg, NS-rep, and S-rep leaves, compared on a leaf area basis. The leaf material examined in this zymogram corresponded to that examined for gene expression (panel A). This figure is available in colour at *JXB* online.

Comparative analysis of AtSASP to other subtilisin-like serine proteases from Arabidopsis *and other flowering plants*

A TAIR-BLASTP search (http://www.arabidopsis.org/Blast) using AtSASP as a query retrieved proteins from the SBT1 subtilase subfamily as *AtSASP* (Rautengarten *et al.*, 2005; Rawlings *et al.*, 2012), followed by members from the SBT5 subfamily (Supplementary Table S1). Gene expression profiles of the BLASTP top 10 closest SASP homologues were surveyed using the eFP Browser Database (Winter *et al.*, 2007) and showed that two out of the 10 hits, the jasmonate-induced AtSBT1.6, SLP2 (Golldack *et al.*, 2003), and AtSBT5.6 subtilase, are mildly upregulated in senescing leaves, whereas the expression of the other proteases remains unchanged or is downregulated during leaf senescence (Supplementary Table S1). Another BLASTP search was performed at the NCBI non-redundant database (www.ncbi.nlm.nih.gov/), excluding *Arabidopsis* sequences. Putative AtSASP orthologues were identified in dicot and monocot crop species (Supplementary Table S2). The wheat subtilase retrieved was recently purified and identified as a senescence-associated protease (Wang *et al.*, 2013), whereas the rice subtilase Os02g779200/LOC_Os02g53860 retrieved in this BLASTP appears as a pairwise orthologue with AtSASP in a cross comparison of *Arabidopsis* and rice Ser-proteases (Tripathi and Sowdhamini, 2006). Subsequently, a multiple sequence alignment was generated by combining selected TAIR and NCBI- BLASTP hits (Supplementary Figure S3), based on which a phylogenetic tree was constructed (Fig. 3). The analysis showed one big group, clustering AtSASP and all its putative orthologues which were included in the alignment. The cluster is later joined by *Arabidopsis* subtilases, either pairwise or separately. Plant subtilisin proteases are characterized

by a large protease-associated (PA) domain between the His and Ser of the catalytic triad, which is predicted to mediate protease–substrate interaction (Mahon and Bateman, 2000). Conserved amino acid residues specific to AtSASP and its putative orthologues locate within the PA domain (Supplementary Figure S3: underlined amino acid residues) and might be related to specific substrate recognition.

Characterization of T-DNA insertion lines: mutant at-sasp *plants show a reproductive development phenotype with increased seed yield*

To study the specific function of AtSASP, two independent T-DNA insertion lines were examined and screened for homozygosity: *sasp-1*, SALK_147962; and *sasp-2*, SALK_063823 (obtained from the ABRC at Ohio State University, http://www.biosci.ohio-state.edu/pcmb/Facilities/abrc/index.html). *AtSASP* is a monocistronic gene, and both *sasp-1* and *sasp-2* alleles carry the T-DNA at the 3′-end of the gene. *AtSASP* gene expression and AtSASP proteolytic activity was examined in *sasp-1* and *sasp-2* mutants. RT-PCR analysis was performed using template RNA extracted from senescing leaves. *AtSASP* transcripts were undetectable in mutant lines (Fig. 4A). Consistent with this result, zymograms carried out with protein samples from the same leaves used for RT-PCR showed no AtSASP proteolytic activity in *sasp-1* and *sasp-2* lines (Fig. 4B). These results confirm that AtSASP is responsible for the senescence-associated proteolytic activity detected in zymograms, but also that *sasp-1* and *sasp-2* are null mutant lines.

Mutant *sasp-1* and *sasp-2* plants are indistinguishable from the wild type at early stages of plant development. In spite of the senescence-associated expression of SASP, *sasp-1* and *sasp-2* did not show a consistent and reproducible effect on leaf senescence. However, during inflorescence development, *sasp-1* and *sasp-2* plants produced more branched main stems than wild-type plants. Regardless of increased branching, parameters such as silique size or seed number per silique and silique number per branch remained the same in wild-type and mutant plants, leading to a mutant phenotype with higher silique production at harvest (when the whole plant is dry) compared to the wild type (Fig. 4C). Interestingly, there was some plasticity in these phenotypic differences between mutants and the wild type when several replicates of phenotypic analysis were observed. For example, silique number increased by 13 to 42% in mutant plants compared to the wild type depending on whether plants were grown at 90 or 150 µmol m^{-2} s^{-1}, respectively (Table 2).

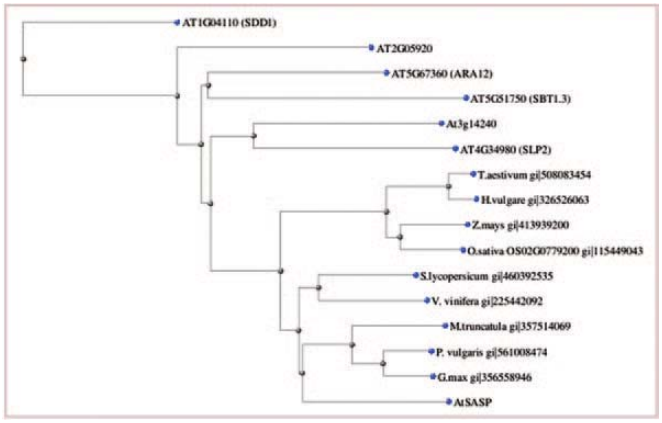

Fig. 3. Rooted tree generated from the multiple sequence alignment of AtSASP, other *Arabidopsis* subtilases (Supplementary Table S1), and subtilases from other flowering plants identified in BLASTP analysis (Supplementary Table S2) using COBALT RID software. This figure is available in colour at *JXB* online.

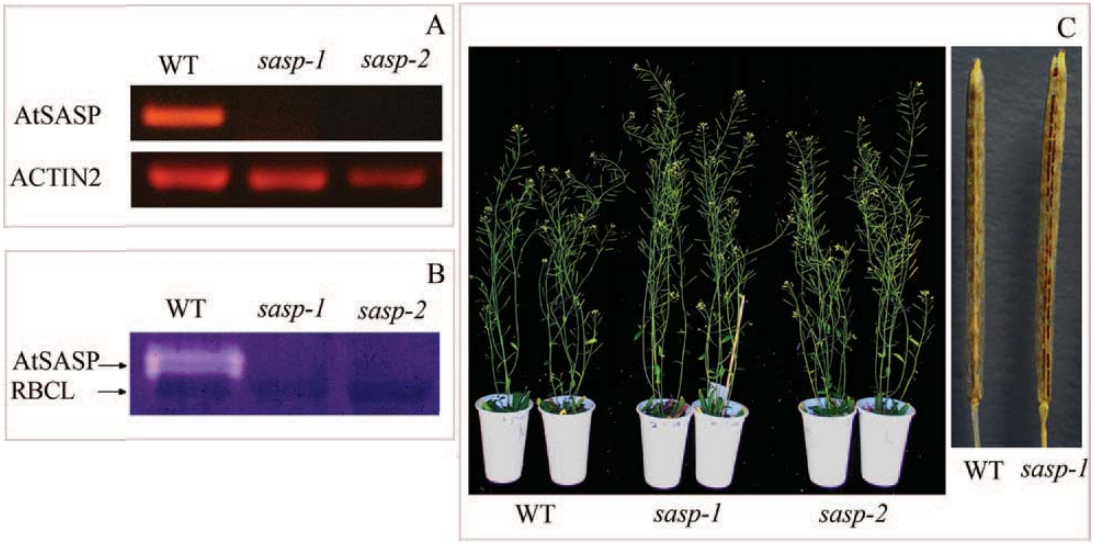

Fig. 4. Molecular and phenotype analysis of *sasp-1* and *sasp-2* T-DNA insertion lines. (A) RT-PCR of *AtSASP* in wild-type (WT), *sasp-1*,and *sasp-2* plants. RNA was extracted from senescing leaves. *ACTIN2* was amplified as a control for equal amounts of RNA. (B) AtSASP activity in senescing leaves of wild-type, *sasp-1*, and *sasp-2* plants. The amount of sample loaded onto the activity SDS-PAGE represents the same leaf area. Rubisco Large Subunit (RBCL) is also indicated as a loading control. (C) Left, and from left to right: wild-type, *sasp-1*, and *sasp-2* plants at reproductive stage growing under a photoperiod of 150 µmol m^{-2} s^{-1}, 16 h light/12 h dark. Right: dehiscent siliques from the main stem of wild-type and *sasp-1* plants. Note that mature seeds become visible through the ripening silique valves. This figure is available in colour at *JXB* online.

Genetic complementation of sasp-1 *with* AtSASP *and with its putative rice orthologue,* OsSASP

To advance the functional analysis of SASP, and to gain insight into the function of its putative orthologues, *sasp-1* plants were complemented either with *AtSASP* or its putative rice orthologue, Os02g779200 (Fig. 3; Supplementary Table S2), hereafter termed *OsSASP*. Considering the potential advantage of using fluorochrome-tagged proteins, translational C-terminal *YFP* fusions of *SASP* expressed under the control of the CaMV35 promoter (35S-AtSASP-YFP and 35S-OsSASP-YFP) were generated for *sasp-1* complementation. Some GFP-C-terminal-tagged plant subtilases are functional (Watanabe *et al.*, 2004; Ramirez *et al.*, 2013), whereas in the case of subtilases which undergo C-terminal processing as a maturation step, such as SDD1, GFP fusions are unstable but GFP does not interfere with protease processing and expression (von Groll *et al.*, 2002). Transgenic lines were obtained from separate transformations, and screened for transcripts, protein expression, and SASP protease activity. RT-PCR analysis of selected AtSASP-YFP and OsSASP-YFP lines confirmed that *AtSASP* or *OsSASP* were expressed in the selected transformed *sasp-1* plants (Fig. 5A). Chimeric proteins in transgenic lines were examined by immunodetection of YFP. Antibodies against GFP recognized a 27 kD fragment in both AtSASP-YFP and OsSASP-YFP lines, which was highly unstable, in particular for the OsSASP-YFP construction, as YFP was only detectable under mild denaturing conditions (Fig. 5B). The released 27 kD fragment containing YFP indicates that AtSASP and OsSASP proteases undergo C-terminal processing. In agreement with these observations, zymograms showed SASP proteolytic activity in AtSASP-YFP-*sasp-1* leaf samples, at the same apparent molecular size as that in wild-type leaf samples (Fig 5C), supporting the immunological evidence that maturation of SASP involved the release of a C-terminal peptide. Non-detection of SASP-like proteolytic activity in OsSASP-YFP-*sasp-1* plants suggests that OsSASP protease might require other optimal conditions (i.e. different pH or cofactors) to show in vitro activity. Zymograms from senescing leaves of wild-type rice did not reveal SASP-like proteolytic activity either, supporting the idea that rice SASP activity may require different zymogram conditions.

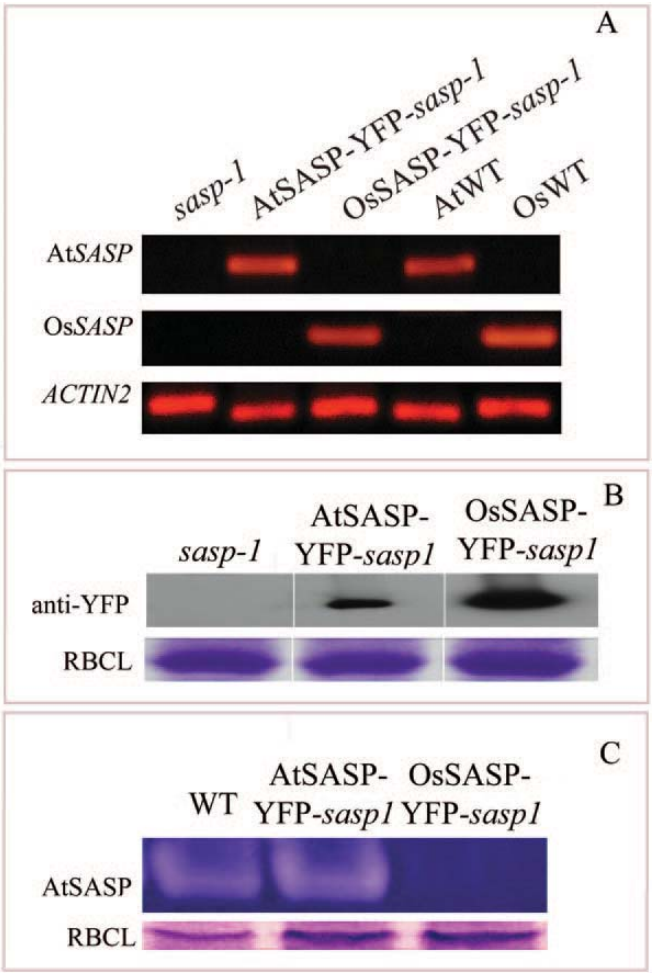

Fig. 5. Molecular analysis of AtSASP-YFP-*sasp-1* and OsSASP-YFP-*sasp-1* plants. (A) RT-PCR of *AtSASP* and Os*SASP* genes in complemented *sasp-1* plants. *ACTIN2* was amplified as a control for equal amounts of RNA. (B) Upper row: immunodetection of YFP in transgenic lines. Lower row: Coomassie blue-stained SDS-PAGE gel showing Rubisco Large Subunit (RBCL) as a protein loading control. (C) Upper row: *SASP* activity detected in leaves of wild-type (WT), AtSASP-YFP-*sasp-1*, and OsSASP-YFP-*sasp-1* plants. Lower panel: Coomassie blue-stained SDS-PAGE gel showing Rubisco Large Subunit as a protein loading control. The amount of sample loaded onto the activity gel represents the same leaf area. This figure is available in colour at *JXB* online.

Constitutive ectopic expression of SASP *in a* sasp-1 *background leads to fewer branched inflorescences and reduced seed yield*

A comparative phenotypic analysis of *sasp-1,* AtSASP-YFP-*sasp-1*, OsSASP-*sasp-1*, and wild-type plants was performed during reproductive development. Under a 16 h light/8 h dark period, and 150 µmol m^{-2} s^{-1} PPFD, all four genotypes flowered within a 4 d interval, and matured ~10 weeks after flowering. The yield-related traits 'reproductive branch number per plant', 'flower and silique number per plant', and plant height were monitored non-destructively over time. Branching pattern was considered as in Guo and Gan (2011), where branches originating directly from the primary stem are designated first order (1BR), those originating from 1BR are referred to as second order (2BR), and so on. Silique distribution was analysed following the same organization, i.e. siliques originating from first, second, or third order branches, or from the terminal inflorescence. Branches and siliques originating from the main stem were considered separately from those originating from axillary stems (stems originating from the axillary bud of rosette leaves), which were pooled together. Branching and silique distribution patterns were determined at harvest along with main stem and axillary stem biomass, and seed size. Fig. 6 shows increased plant size in *sasp-1*, compared to wild-type and complemented lines by mid-reproductive phase, 36 d after flowering (DAF). The total number of branches per plant did not differ significantly among genotypes early after flowering, even though *sasp-1* plants tended to develop a higher number of branches per plant. This trend increased

Fig. 6. Phenotype of *sasp-1*, AtSASP-YFP-*sasp-1*, OsSASP-*sasp-1*, and wild-type (WT) plants at 36 DAF growing under long day conditions. This figure is available in colour at *JXB* online.

during the reproductive period, leading to 25% more branches per plant in *sasp-1* plants at harvest compared to the wild type, AtSASP-YFP-*sasp-1*, and OsSASP-*sasp-1*, which displayed a similar number of branches per plant (Fig. 7A). The number of flowers and siliques per plant was higher in *sasp-1* compared to the rest of the lines, particularly at early stages (8 and 18 DAF) when *sasp-1* had 60% more flowers than the lines with a functional *SASP* gene (Fig. 7B). By 36 DAF the silique set remained higher in *sasp-1* compared to the other lines, but the difference declined (from 60 to 24%) as silique production increased in all genotypes. At maturity (71 DAF), silique number was ~25% higher in *sasp-1*, compared to wild-type and AtSASP-YFP-*sasp-1* lines, and ~35% higher compared to OsSASP-*sasp-1*. A similar trend was observed in plant height: *sasp-1* plants were 17% taller than the other lines at 36 DAF, but thereafter this difference decreased over time as the maximum plant height was eventually reached by all four genotypes (Fig. 7C). The timing of formation, and the final number of axillary stems per plant was variable within plants from the same line, and no differences were observed among genotypes. Indeed, the relative contribution of the main stem and axillary stem to the total number of branches and siliques produced per plant at harvest was conserved among genotypes (Fig.7D and E), i.e. the number of flowers and siliques increased in *sasp-1* in both the main stem and the axillary stems. This observation is consistent with dry mass data that shows a similar main stem/axillary stem biomass ratio (around 72–80%) in all the genotypes (Fig. 7F). Biomass accumulation was significantly higher in *sasp-1* compared to the wild type and AtSASP-YFP-*sasp-1* by ~19%, and by about 28% with respect to OsSASP-*sasp-1* plants.

All genotypes developed up to 4BR, but these represented <2% of total branches per plant. No differences among genotypes were observed in 1BR, whereas *sasp-1* developed 14% more 2BR than the wild type and AtSASP-YFP-*sasp-1*, and 20% more than OsSASP-*sasp-1* (Fig. 7G). A similar pattern was observed for 3BR, even though they did not differ significantly due to the high variation in 3BR/plant ratio within genotypes. Silique distribution pattern resembled branching patterns (Fig. 7H). The number of siliques in first order branches, and in the terminal inflorescence, was similar in all genotypes, whereas the number in second and third order branches was 12–14% higher in *sasp-1* compared to the wild type and around 22% higher compared to AtSASP-YFP-*sasp-1* and OsSASP-YFP-*sasp-1*. The increased silique set in *sasp-1* was mainly due to the increased number of BR2 and BR3, as the silique number/branch ratio in each order branch was the same among genotypes. No effect was observed for seed set per silique, but seeds produced by *sasp-1* were 5% smaller than those produced by wild-type and complemented lines (Fig. 7I and J).

Overall, this analysis demonstrated that the inactivation of *AtSASP* resulted in a higher growth rate of developing inflorescences that led to an increase in final branching of the main stem. As the silique number/Branch ratio remained unchanged there is an increase in the final seed number at yield, accompanied by a partial reduction in seed size. The restoration of the wild-type phenotype in *sasp-1* by ectopic expression of AtSASP or OsSASP confirmed the involvement of the subtilisin protease in the modulation of reproductive development

Discussion

Detection, identification, and expression analysis of SBT1.4/AtSASP

In this work, activity-based protease detection was combined with proteomic techniques to detect and identify proteases with activities associated with leaf senescence.

AtSASP was detected through zymography and observed to increase in activity during *Arabidopsis* leaf senescence. The SDS-PAGE-based zymography used in this approach only allows for the detection of proteases that are able to renature and remain active after 1D or 2D activity gel electrophoresis; these are mainly monomeric, SDS-stable proteases. Another drawback of SDS-PAGE-based zymography is that pro-proteases and originally inactive proteases might become catalytically activated (i.e autocatalytic pH-dependent activation: Rose *et al.*, 2010; Vandooren *et al*, 2013), and therefore the observation of an increase in activity might be an artifact. Nevertheless, all the AtSASP peptides identified by mass spectrometry locate within the mature protein region (Fig. 1C) and, since no peptides corresponding to the propeptide domain were detected, it was surmised that SASP was already mature and active *in vivo*, before zymogram analysis.

The doublet band of activity detected in our zymograms corresponding to the same gene product could be related to posttranslational modifications. AtSASP was identified in the proteome of N-glycosylated stem cell wall proteins (Minic *et al.*, 2007), suggesting that AtSASP forms might represent

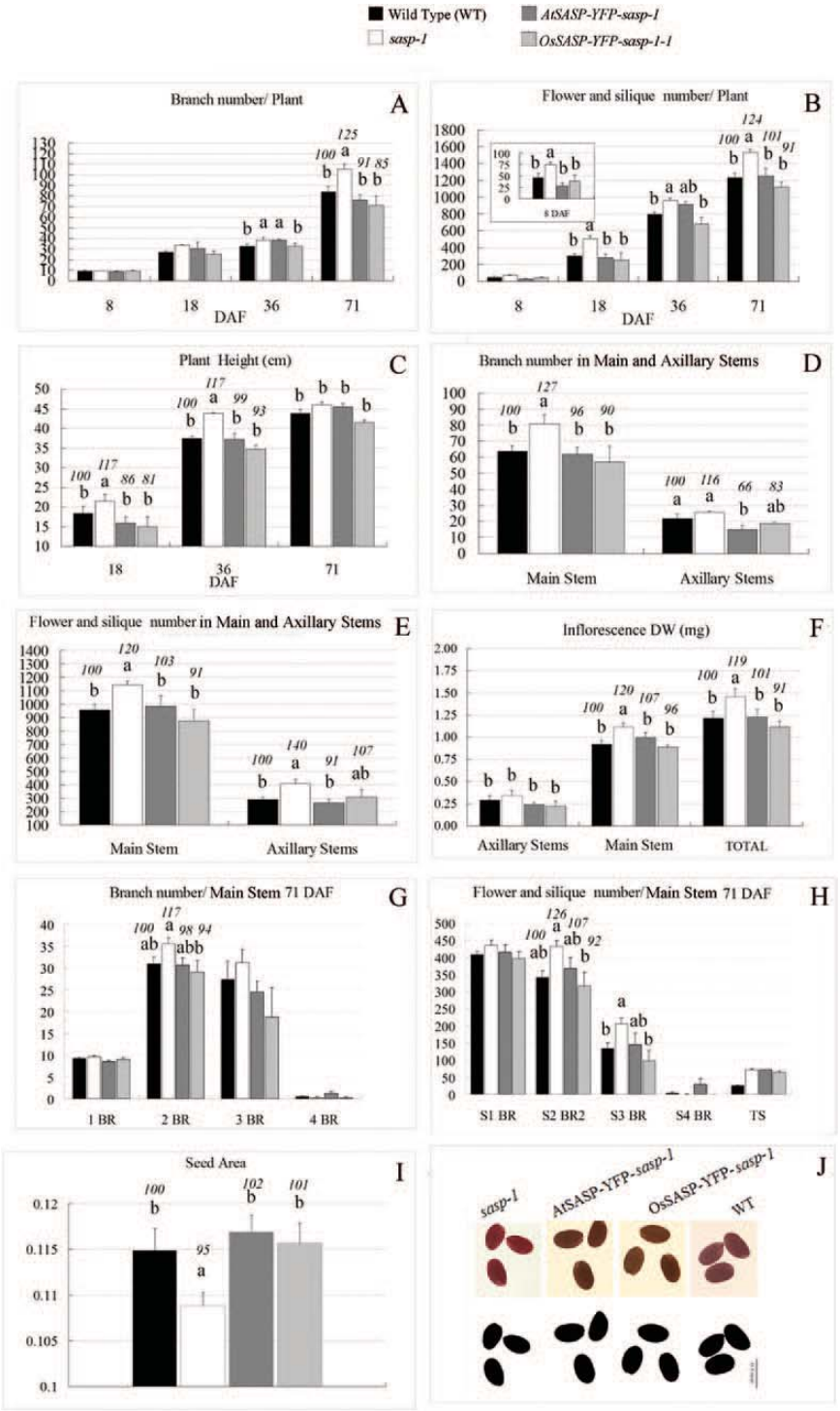

Fig. 7. Yield-related trait analysis of AtSASP- and OsSASP-complemented *sasp-1* plants. (A) Number of inflorescence branches per plant (*y* axis) over reproductive development ($n = 22$). (B) Number of flowers and siliques per plant (*y* axis) over reproductive development ($n = 22$). (C) Plant height (*y* axis) over reproductive development. Values represent the average length of the main stem terminal inflorescence ($n = 22$). (D) Number of inflorescence branches on the main and axillary stems per plant at harvest. (E) Number of flowers and siliques on the main and axillary stems at harvest. (F) Inflorescence dry biomass at harvest. The graph shows total dry weight (DW) or DW discriminated between the main and axillary stems. (G) Branching pattern on the main stem at harvest. (H) Branching pattern-related silique distribution on the main stem at harvest. (I and J) Average transverse area of seeds collected from ripening siliques originating from the terminal inflorescence of the main stem ($n = 70$). Seeds were software analysed (I) for seed area quantification, and the bar graph shows average seed area; error bars depict SE. Numbers above columns indicate percentage compared to wild type, which was considered 100%. Letters indicate significant differences between genotypes ($P < 0.05$). This figure is available in colour at *JXB* online.

different levels of N-glycosylation. AtSASP was also detected in the proteome of the leaf extracellular fluid (Boudart *et al.*, 2005). The experimental data on AtSASP apoplastic location is consistent with bioinformatic predictions, and this is a shared characteristic of most plant subtilases (Berger and Altmann, 2000; Beers *et al.*, 2003). In addition, AtSASP was

detected in the proteome of central vacuoles isolated from leaves of vegetative *Arabidopsis* (Carter *et al.*, 2004) which opens up the possibility that changes in AtSASP subcellular location(s) might take place during senescence.

Leaf senescence-associated, subtilisin-like protease activity was also detected and characterized in wheat (Roberts *et al.*, 2003; Roberts *et al.*, 2006), and a wheat senescence upregulated subtilase with high amino acid sequence homology to AtSASP and similar *in gel* activity was recently identified and characterized (Wang *et al.*, 2013). AtSASP activity was also detected in other above-ground photosynthetic organs, but not in roots. *AtSASP* expression increases during leaf senescence in an organ- and plant age-dependent manner (Fig. 2). Experimental information on *AtSASP* expression has also been also reported in van der Graaff *et al.* (2006). The authors identified senescence-associated genes and examined their relative expression under developmental and dark-induced senescence of individual leaves attached to or detached from the plant. In these experiments *AtSASP* expression increased 2.1-fold in a 2 week time period during developmental senescence, whereas *AtSASP* transcripts increased 1.3-fold when leaf chlorophyll decreased to 75%. *AtSASP* expression increased 1.8-fold during dark-induced senescence of attached leaves, whereas in detached leaves expression remained unchanged (van der Graaff *et al.*, 2006; Supplementary Table S2). Taken together, these results demostrate that *AtSASP* expression in leaves is partially autonomous and closely associated with the developmental stage and age of the plant.

SASP *expression affects plant development and yield*

AtSASP loss of function leads to rapid elongation of the main shoot, increased inflorescence branching and biomass, higher silique number at maturity, and slightly reduced seed size. Constitutive ectopic expression of *AtSASP* or its rice orthologue Os*SASP* in a *sasp-1* background leads to plants with fewer branches and reduced inflorescence biomass, fewer siliques at harvest, and wild-type seed size (Fig. 6). These results indicate that *sasp-1* plants were functionally complemented by either 35S:AtSASP-YFP-*sasp-1* or 35S:OsSASP-YFP-*sasp-1* constructs. In addition, immunodetection analysis of YFP from 35S:AtSASP-YFP-*sasp-1* and 35S:OsSASP-YFP-*sasp-1* leaf extracts indicates that AtSASP and OsSASP are C-terminally cleaved in their protein maturation process.

Inactivation of *AtSASP* by T-DNA insertion lead to a 24% increase in silique yield at harvest compared to wild-type or AtSASP and OsSASP complemented plants. The seed number/silique ratio is not affected by the increased silique set, but a partial compensation effect is observed on seed size, which is 5.0% smaller in *sasp-1* compared to the wild-type and complemented lines (Fig. 7I). The enhanced silique production does not seem to be related to changes in the whole inflorescence architecture, as no substantial differences were observed in the timing of formation and final number of axillary stems among *sasp-1* and AtSASP-YFP-*sasp-1* and OsSASP-YFP-*sasp-1* lines. The branching pattern on the main stem was similar across all the genotypes, which developed up to 4BR. In *sasp-1*, the number of BR2 and BR3 particularly increased compared to wild-type and complemented lines (Fig. 7G). The higher number of BR2 and BR3 led to an increased silique set per main stem in *sasp-1,* which is 12–14% higher than the wild type and around 22% higher compared to the AtSASP-YFP-*sasp-1* and OsSASP-YFP-*sasp-1* lines. The time-course analysis of branch production reveals statistically significant differences between *sasp-1* and the rest of the genotypes by the middle stage of the reproductive phase, after BR2 developed on the main stem, whereas differences in silique production were already observed at earlier stages of inflorescence development, when the number of flowers and siliques developed by *sasp-1* plants was up to 60% higher than in wild-type and complemented lines. Thereafter, this difference narrowed down to 24% by the middle stage of the reproductive phase (Fig. 7A). A similar pattern of branch and silique production was observed in *aap2* (*Amino Acid Permease* 2; AAP2) mutant plants, which are defective in xylem-phloem transfer of amino acids (Zhang *et al.*, 2010).

The development of reproductive structures is the result of complex interaction between different endogenous and environmental factors, i.e. maintenance of meristem identity, local and long-distance regulation of bud activity and outgrowth, sink/source ratios, interbranch and/or intershoot competition, resource allocation between fruits, organ growth rate, light quality and quantity, and nutrient availability (Nooden and Penney 2001; Aguilar-Martınez *et al.*, 2007; Ongaro *et al.*, 2008; Crawford *et al.*, 2010; Beveridge and Kyozuka, 2010; Domagalska and Leyser, 2011), with a large degree of plasticity as an outcome of such complexity. A variety of gene mutations led to altered inflorescence development. For instance, the phloem-localized AAP2 is involved in the long-distance transport pathway for amino acids. Changes in source/sink translocation of amino acids occur in *aap2* plants that develop increased branch and silique numbers and seeds with lower nitrogen content, with a net increase in seed yield (Zhang *et al.*, 2010). Hormonal regulation of shoot branching was robustly revealed through the study of 'bushy' mutants. Overbranched phenotypes such as *supershoot* and *at-myb2* resulted from an effect on the negative control over cytokinin-mediated promotion of bud outgrowth (Crawford *et al.*, 2010; Guo and Gan, 2011). Increased axillary stems are usually related to deficiencies in strigolactone and the auxin-mediated, long-distance MAX/RMS/D pathway of bud outgrowth regulation, conserved in *Arabidopsis* (*max*), petunia (*rms*), rice (*d*), and other species (reviewed in Leyser, 2009; Waldie *et al.*, 2014). Interestingly, *MAX2*, a key gene in the MAX/RMS/D pathway, encodes an F-box regulator previously described as the leaf senescence-associated gene *ORE9*, due to the delayed senescence exhibited by *ore9* plants (Woo *et al.*, 2001). The *max2* overbranched inflorescence is similar to that of *gat1* (alutamine amidotransferase, GAT1). GAT1 expression is high in flowers and siliques, and is repressed by long-term nitrogen deficit. Both *max2* and *gat1* exhibit enhanced branching independently of nitrogen availability (Zhu and Kranz, 2012).

Regardless of the mutation that causes more branched *Arabidopsis* plants, there seems to be a link between increased

branching and retarded monocarpic senescence. This could be related to a delay in post-mitotic senescence (Gan, 2003) in more branched phenotypes, which behave as more indeterminate plants, like *supershoot* and *at-myb2* (Tantikanjana *et al.*, 2001; Guo and Gan, 2011). On the other hand, the photosynthetic stems of *Arabidopsis* contribute to carbon gain, and indeed carbon assimilation in the inflorescence (stems, cauline leaves, and silique valves) continues after rosette senescence (Earley *et al.*, 2009). More branched plants might produce more photoassimilates and/or prolong the photosynthetic period. Interestingly, the *sasp-1* phenotype is stronger under higher (150 µmol m^{-2} s^{-1}) than lower irradiance (90 µmol m^{-2} s^{-1}), with a 2-fold increase in branch and silique production (Fig. 4). Correlative inhibition effects may also play an important role. More branched phenotypes are often related to lower seed yield or even infertility (Tantikanjana *et al.*, 2001; Footitt *et al.*, 2007). Increased branching as a consequence of partial or total infertility cannot be ruled out (Bleecker and Patterson, 1997). By contrast, there are few examples such as *sasp-1* and *aap2* which develop more branched but fertile inflorescences bearing more normal sized siliques and viable seeds. However, there is a partial compensation effect on seed size in *sasp-1* plants. Although seed number is usually negatively correlated with seed size, it is considered an important yield-contributing parameter for most crops (Diepenbrock, 2000; Peltonen-Sainio *et al.*, 2007).

AtSASP and OsSASP: evidence of a conserved regulatory mechanism in reproductive development?

The fact that constitutive expression of Os*SASP* in *sasp-1* complemented it to the wild-type phenotype reinforces the possibility that Os*SASP* is the rice orthologue of *AtSASP*. Cross species complementation suggests at least partial conservation of SASP function between distant species. Conserved regulatory mechanisms between dicots and monocots using *Arabidopsis* and rice as models have been elucidated. The genetic mechanisms of meristem identity, maintenance, and dormancy are partially conserved between *Arabidopsis* and grasses such as maize and rice (see review in Pautler *et al.*, 2013), as is the hormonal regulation of branching (Lin *et al*, 2009; Cardoso *et al.*, 2014). Furthermore, the loss of function of the rice gene homologue to *MAX2*/*ORE9*, *DWARF3*, also leads to delayed leaf senescence and death in rice (Yan *et al.*, 2007). Other examples, however, demonstrate lower degrees of conservation. *GW2*, a RING-type protein of the ubiquitin-proteasome pathway, was shown to control rice grain width and weight (Song *et al.*, 2007). The overexpression of AT1G78420, one of the two putative orthologues of GW2 in *Arabidopsis*, resulted in plants with increased number of siliques but normal seed size (Van Daele *et al.*, 2012).

SASP-specific function in the context of known subtilisin-like proteases

The *Arabidopsis* genome encodes 56 subtilases, and even though most homozygous knockout mutants do not show obvious distinguishable phenotypes under standard conditions (Rautengarten *et al.*, 2005), detailed functional analysis has revealed specific functions in many cases. Most of the known subtilisin proteases are expressed as protease precursors that are directed to the endomembrane system and extracellular space. The extracellular SDD1 (*Stomatal Density and Distribution1*) subtilase controls stomatal distribution and density (Berger and Altmann, 2000). ALE1 (*Abnormal leaf Shape 1*) participates in cuticle formation and epidermal differentiation (Watanabe *et al.*, 2004). SDD1 and ALE1 are suggested to generate peptide signals required for proper differentiation of the epidermis (Tanaka *et al.*, 2001, von Groll *et al.*, 2002). Other subtilisin proteases are involved in seed development (Rautengarten *et al.*, 2008), root branching (Neuteboom *et al.*, 1999) and signalling related to stress responses (Tornero *et al.*, 1996; Srivastava *et al.*, 2008). In summary, most of the characterized plant subtilisin proteases function in signalling pathways related to development and stress responses. SASP could be involved in the processing of an extracellular or plasma membrane located target or the release of an apoplastic signal, repressing inflorescence branching and silique production as reproductive development and senescence proceeds, thereby minimizing inter-branch or inter-fruit competition for resources.

Supplementary material

Supplementary data can be found at *JXB* online.

Supplementary Table S1. **C**omparison of AtSASP to other *Arabidopsis* subtilisin proteases. AtSASP BlastP 10 top hits (TAIR BLASTP 2.2.17) with bit scores and *E*-values are shown. The corresponding gene expression during leaf senescence for each protein was classified as unchanged, down or up regulated based on eFP Browser developmental stage expression DNA microarrays analysis.

Supplementary Table S2. **C**omparison of AtSASP to subtilisin proteases from different flowering plants. NCBI-BLASTP search on the non-redundant (nr) database (www.ncbi.nlm.nih.gov) excluding *Arabidopsis* sequences. Percentage Covered and Maximal identity retrieved in the search are shown.

Supplementary Table S3. List of primers used in this work.

Supplementary Figure S1. Pictogram illustrating the developmental stage-specific expression of *AtSASP*, extracted from the eFP Browser Microarrays Database.

Supplementary Figure S2. Detection of AtSASP activity *in vitro* in roots, rosette and cauline leaves, main inflorescence stem, inflorescence branches, and non-senescent and senescent (yellowing) siliques.

Supplementary Figure S3. Multiple amino acid sequence alignment of AtSASP to other subtilisin-like serine proteases from *Arabidopsis* (Supplementary Table S1) and other flowering plant species identified in an NCBI BLASTP analysis (Supplementary Table S2) using COBALT RID.

Funding

This work was supported by grants from the Consejo Nacional de Investigaciones Científicas y Técnicas (CONICET) Argentina, (PIP 0487-2009), Agencia Nacional de Promoción

Científica y Tecnológica, Argentina, (PICT 0061-2008), and Collaborative Project SECTIP/Academy of Finland (FI/PA02/ BO2, 2003- 2005). E-MA, NB and ET were supported by Academy of Finland.

Acknowledgements

Thanks are due to Dr. F. Chirdo for the use of the iCycler real time PCR, Ms. Mariela Bayardo for technical assistance and Drs. Silvana Petruccelli, Facundo Gomez and Jan Chojecki for their helpful comments.

References

Aguilar-Martınez JA, Poza-Carrion C, Cubas P. 2007. Arabidopsis BRANCHED1 acts as an integrator of branching signals within axillary buds. *The Plant Cell* **19,** 458–472.

Beers EP, Jones AM, Dickerman AW. 2003. The S8 serine, C1A cysteine, and A1 aspartic protease families in Arabidopsis. *Phytochemistry* **65,** 43–48.

Berger D, Altmann T. 2000. A subtilisin-like serine protease involved in the regulation of stomatal density and distribution in Arabidopsis thaliana. *Genes and Development* **14,** 1119–1131.

Beveridge CA, Kyozuka J. 2010. New genes in the strigolactone-related shoot branching pathway. *Current Opinion in Plant Biology* **13,** 34–39.

Bleecker AB, Patterson SE. 1997. Last exit, senescence, abscission, and meristem arrest in Arabidopsis. *The Plant Cell* **9,** 1169–1179.

Boudart G, Jamet E, Rossignol M, Lafitte C, Borderies G, Jauneau A, Pont-Lezica R. 2005. Cell wall proteins in apoplastic fluids of Arabidopsis thaliana rosettes, identification by mass spectrometry and bioinformatics. *Proteomics* **5,** 212–221.

Buchanan-Wollaston V, Earl S, Harrison E, Mathas E, Navabpour S, Page T, Pink D. 2003. The molecular analysis of leaf senescence–a genomics approach. *Plant Biotechnology* **1,** 3–22.

Cardoso C, Zhang Y, Jamil M, Hepworth J, Charnikhova T, Dimkpa SO, Ruyter-Spira C. 2014. Natural variation of rice strigolactone biosynthesis is associated with the deletion of two MAX1 orthologs. *Proceedings of the National Academy of Sciences, USA* **111,** 2379–2384.

Carter C, Pan S, Zouhar J, Avila E L, Girke T, Raikhel NV. 2004. The vegetative vacuole proteome of Arabidopsis thaliana reveals predicted and unexpected proteins. *The Plant Cell* **16,** 3285–3303.

Chardon F, Noël V, Masclaux-Daubresse C. 2012. Exploring NUE in crops and in Arabidopsis ideotypes to improve yield and seed quality. *Journal of Experimental Botany* **63,** 3401–3412.

Chung DM, Kim KE, Ahn KH *et al.* 2011. Silver-stained fibrin zymography, separation of proteases and activity detection using a single substrate-containing gel. *Biotechnology Letters* **33,** 1663–1666.

Clough SJ, Bent AF. 1998. Floral dip, a simplified method for Agrobacterium-mediated transformation of Arabidopsis thaliana. *The Plant Journal* **16,** 735–43.

Coffeen WC, Wolpert TJ. 2004. Purification and characterization of serine proteases that exhibit caspase-like activity and are associated with programmed cell death in Avena sativa. *The Plant Cell* **16,** 857–873.

Crawford S, Shinohara N, Sieberer T, Williamson L, George G, Hepworth J, Leyser O. 2010. Strigolactones enhance competition between shoot branches by dampening auxin transport. *Development* **137,** 2905–2913.

Delorme VG, McCabe PF, Kim DJ, Leaver CJ. 2000. A matrix metalloproteinase gene is expressed at the boundary of senescence and programmed cell death in cucumber. *Plant Physiology* **123,** 917–927.

Diepenbrock W. 2000. Yield analysis of winter oilseed rape (Brassica napus L.), a review. *Field Crops Research* **67,** 35–49.

Domagalska MA, Leyser O. 2011. Signal integration in the control of shoot branching. *Nature Reviews Molecular Cell Biology* **12,** 211–221.

Earley EJ, Ingland B, Winkler, Tonsor SJ. 2009. Inflorescences contribute more than rosettes to lifetime carbon gain in Arabidopsis thaliana (Brassicaceae) *American Journal of Botany* **96,** 786–792.

Eason JR, Ryan DJ, Watson LM, Hedderley D, Christey MC, Braun RH, Coupe SA. 2005. Suppression of the cysteine protease, aleurain, delays floret senescence in Brassica oleracea. *Plant Molecular Biology* **57,** 645–657

Footitt S, Cornah JE, Pracharoenwattana I, Bryce JH, Smith SM. 2007. The Arabidopsis 3-ketoacyl-CoA thiolase-2 (kat2-1) mutant exhibits increased flowering but reduced reproductive success. *Journal of Experimental Botany* **58,** 2959–2968.

Gan S. 2003. Mitotic and postmitotic senescence in plants. *Science* **38b** 7.

Golldack D, Popova OV, Dietz KJ. 2002. Mutation of the matrix metalloproteinase At2-MMP inhibits growth and causes late flowering and early senescence in Arabidopsis. *The Journal of Biological Chemistry* **277,** 5541–5547.

Golldack D, Vera P, Dietz KJ. 2003. Expression of subtilisin-like serine proteases in Arabidopsis thaliana is cell-specific and responds to jasmonic acid and heavy metals with developmental differences. *Physiologia Plantarum* **118,** 64–73.

Gregersen PL, Culetic A, Boschian L, Krupinska K. 2013. Plant senescence and crop productivity. *Plant Molecular Biology* **82,** 603–622.

Grudkowska M, Lisik P, Rybka K. 2013. Two-dimensional zymography in detection of proteolytic enzymes in wheat leaves. *Acta Physiolologiae Plantarum* **35,** 3477–3482.

Gu C, Shabab M, Strasser R, Wolters PJ, Shindo T. Niemer M, van der Hoorn RA. 2012. Post-translational regulation and trafficking of the granulin-containing protease RD21 of Arabidopsis thaliana. *PLoS ONE* **7,** e32422.

Guo Y, Cai Z, Gan S. 2004. Transcriptome of Arabidopsis leaf senescence. *Plant, Cell and Environment* **27,** 521–549.

Guo Y, Gan S. 2011. AtMYB2 regulates whole plant senescence by inhibiting cytokinin-mediated branching at late stages of development in Arabidopsis. *Plant Physiology* **156,** 1612–1619.

Kato Y, Murakami S, Yamamoto Y, Chatani H, Kondo Y, Nakano T, Yokota A, Sato F. 2004. The DNA-binding protease, CND41, and the degradation of ribulose-1,5-bisphosphate carboxylase/oxygenase in senescent leaves of tobacco. *Planta* **220,** 97–104.

Kato Y, Yamamoto Y, Murakami S, Sato F. 2005. Post-translational regulation of CND41 protease activity in senescent tobacco leaves. *Planta* **222,** 643–651.

Laemmli, UK. 1970. Cleavage of structural proteins during the assembly of the head of bacteriophage T4. *Nature* **227,** 680–685.

Leyser O. 2009. The control of shoot branching, an example of plant information processing. *Plant, Cell and Environment* **32,** 694–703.

Lin H, Wang R, Qian Q, Yan M, Meng X, Fu Z, Wang Y. 2009. DWARF27, an iron-containing protein required for the biosynthesis of strigolactones, regulates rice tiller bud outgrowth. *The Plant Cell* **21,** 1512–1525.

Mahon P, Bateman A. 2000. The PA domain, a protease-associated domain. *Protein Science* **9,** 1930–1934.

Martinez D, Bartoli C, Vojislava G, Guiamét JJ. 2007. Vacuolar cysteine proteases of wheat (Triticum aestivum L) are common to leaf senescence induced by different factors. *Journal of Experimental Botany* **58,** 1099–1107.

Martínez DE, Guiamet JJ. 2014. Senescence-related changes in the leaf apoplast. *Journal of Plant Growth Regulation* **33,** 44–55.

Minic Z, Jamet E, Negroni L, der Garabedian PA, Zivy M, Jouanin L. 2007. A sub-proteome of Arabidopsis thaliana mature stem strapped on concanavalin A is enriched in cell wall glycoside. *Journal of Experimental Botany* **58,** 2503–2512.

Nakano T, Murakami S, Yoshid S, Yamada Y, Sato F. 1997. A novel protein with DNA binding activity from tobacco chloroplast nucleoids. *The Plant Cell* **9,** 1673–1682.

Nelson BK, Cai X, Nebenführ A. 2007. A multicolored set of in vivo organelle markers for co-localization studies in Arabidopsis and other plants. *The Plant Journal* **51,** 1126–1136.

Neuteboom LW, Veth-Tello LM, Clijdesdale OR, Hooykaas PJ, van der Zaal BJ. 1999. A novel subtilisin-like protease gene from Arabidopsis thaliana is expressed at sites of lateral root emergence. *DNA Research* **6,** 13–19.

Noodén LD, Guiamet JJ, John I. 2004. Whole plant senescence. In, Noodén LD, ed. *The plant cell death processes*. San Diego, CA, USA: Academic Press, 227–244.

Nooden LD, Penney JP. 2001. Correlative controls of senescence and plant death in Arabidopsis thaliana (Brassicaceae). *Journal of Experimental Botany* **364,** 2151–2159.

Ongaro V, Bainbridge K, Williamsona L, Leyser O. 2008. Interactions between axillary branches of Arabidopsis. *Molecular Plant* **1,** 388–400.

Otegui MS, Noh YS, Martinez DE, Vila Petroff MG, Staehelin LA, Amasino RM, Guiamet JJ. 2005. Senescence-associated vacuoles with intense proteolyticactivity develop in leaves of Arabidopsis and soybean. *The Plant Journal* **41,** 831–844.

Papadopoulos JS, Agarwala R. 2007. COBALT, constraint-based alignment tool for multiple protein sequences. *Bioinformatics* **23,** 1073–1079.

Paparelli E, Gonzali S, Parlanti S, Novi G, Giorgi F M, Licausi F, Perata P. 2012. Misexpression of a chloroplast aspartyl protease leads to severe growth defects and alters carbohydrate metabolism in Arabidopsis. *Plant Physiology* **160,** 1237–1250.

Parrott DL, Martin JM, Fischer AM. 2010. Analysis of barley (Hordeum vulgare) leaf senescence and protease gene expression, a family C1A cysteine protease is specifically induced under conditions characterized by high carbohydrate, but low to moderate nitrogen levels. *New Phytologist* **187,** 313–331.

Pautler M, Tanaka W, Hirano HY, Jackson D. 2013. Grass meristems I, shoot apical meristem maintenance, axillary meristem determinacy and the floral transition. *Plant and Cell Physiology* **54,** 302–312.

Peltonen-Sainio P, Kangas A, Salo Y, Jauhiainen L. 2007. Grain number dominates grain weight in temperate cereal yield determination, Evidence based on 30 years of multi-location trails. *Field Crops Research* **100,** 179–188.

Ramírez V, López A, Mauch-Mani B, Gil MJ, Vera P. 2013. An extracellular subtilase switch for immune priming in Arabidopsis. *PLoS Pathogens* **9,** e1003445.

Rautengarten C, Steinhauser D, Büssis D, Stintzi A, Schaller A, Kopka J, Altman T. 2005. Inferring hypotheses on functional relationships of genes, analysis of the Arabidopsis thaliana subtilase gene family. *PLoS Computational Biology* **4,** e40.

Rautengarten C, Usadel B, Neumetzler L, Hartmann J, Büssis D, Altmann T. 2008. A subtilisin-like serine protease essential for mucilage release from Arabidopsis seed coats. *The Plant Journal* **54,** 466–480.

Rawlings ND, Barrett AJ, Bateman A. 2012. MEROPS, the database of proteolytic enzymes, their substrates and inhibitors. *Nucleic Acids Research* **40,** D343–D350.

Roberts IN, Caputo C, Criado MV, Funk C. 2011. Senescence-associated proteases in plants. *Physiologia Plantarum* **145,** 130–139.

Roberts IN, Murray PF, Caputo CP, Passeron S, Barneix AJ. 2003. Purification and characterization of a subtilisin-like serine protease induced during the senescence of wheat leaves. *Physiologia Plantarum* **118,** 483–490.

Roberts IN, Passeron S, Barneix AJ. 2006. The two main endoproteases present in dark-induced senescent wheat leaves are distinct subtilisin-like proteases. *Planta* **224,** 1437–1447.

Rojo E, Zouhar J, Carter C, Kovaleva V, Raikhel NV. 2003. A unique mechanism for protein processing and degradation in Arabidopsis thaliana. *Proceedings of the National Academy of Sciences, USA* **10,** 7389–7394.

Rose R, Schaller A, Ottmann C. 2010. Structural features of plant subtilases. *Plant Signaling and Behavior* **5,** 180–183.

Rossano R, Larocca M, Riccio P. 2011. 2-D zymographic analysis of Broccoli (Brassica oleracea L. var. Italica) florets proteases, follow up of cysteine protease isotypes in the course of post-harvest senescence. *Journal of Plant Physiology* **168,** 1517–1525.

Sanchez OL, Carbajosa VJ. 2008. DNA-free RNA isolation protocols for Arabidopsis thaliana, including seeds and siliques. *BMC Research Notes* **1,** 93.10.1186/1756-0500-1-93.

Shevchenko A, Wilm M, Vorm O, Mann M. 1996. Mass spectrometric sequencing of proteins silver-stained polyacrylamide gels. *Analytical Chemistry* **68,** 850–858.

Song XJ, Huang W, Shi M, Zhu M Z, Lin HX. 2007. A QTL for rice grain width and weight encodes a previously unknown RING-type E3 ubiquitin ligase. *Nature Genetics* **39,** 623–630.

Srivastava R, Liu JX, Howell SH. 2008. Proteolytic processing of a precursor protein for a growth-promoting peptide by a subtilisin serine protease in Arabidopsis. *The Plant Journal* **56,** 219–227.

Tanaka H, Onouchi H, Kondo M, Hara-Nishimura I, Nishimura M, Machida C, Machida Y. 2001. A subtilisin-like serine protease is required for epidermal surface formation in Arabidopsis embryos and juvenile plants. *Development* **128,** 4681–4689.

Tantikanjana T, Yong JWH, Stuart Letham D, Griffith M, Hussain M, Ljung K, Sandberg G, Sundaresan V. 2001. Control of axillary bud initiation and shoot architecture in Arabidopsis through the SUPERSHOOT gene. *Genes and Development* **15,** 1577–1588.

Tornero P, Conejero V, Vera P. 1996. Primary structure and expression of a pathogen-induced protease (PR-P69) in tomato plants, similarity of functional domains to subtilisin-like endoproteases. *Proceedings of the National Academy of Sciences, USA* **93,** 6332–6337.

Tripathi LP, Sowdhamini R. 2006. Cross genome comparisons of serine proteases in Arabidopsis and rice. *BMC Genomics* **7,** 200.

Van Daele I, Gonzalez N, Vercauteren I, de Smet L, Inzé D, Roldán-Ruiz I, Vuylsteke M. 2012. A comparative study of seed yield parameters in Arabidopsis thaliana mutants and transgenics. *Plant Biotechnology Journal* **10,** 488–500.

van der Graaff E, Schwacke R, Schneider A, Desimone M, Flügge UI, Kunze R. 2006. Transcription analysis of Arabidopsis membrane transporters and hormone pathways during developmental and induced leaf senescence. *Plant Physiology* **141,** 776–792.

Vandooren J, Geurts N, Martens E, Van den Steen PE, Opdenakker G. 2013. Zymography methods for visualizing hydrolytic enzymes. *Nature Methods* **10,** 211–210.

Vartapetian AB, Tuzhikov AI, Chichkova NV, Taliansky M, Wolpert T. 2011. A plant alternative to animal caspases, subtilisin-like proteases. *Cell Death and Differentiation* **18,** 1289–1297.

von Groll U, Berger D, Altmann T. 2002 The subtilisin-like serine protease SDD1 mediates cell-to-cell signaling during Arabidopsis stomatal development. *The Plant Cell*. **14,** 1527–1539.

Wagstaff C, Leverentz MK, Griffiths G, Thomas B, Chanasut U, Stead AD, Rogers HJ. 2002. Cysteine protease gene expression and proteolytic activity during senescence of Alstroemeria petals. *Journal of Experimental Botany* **53,** 233–240.

Waldie T, McCulloch H, Leyser O. 2014. Strigolactones and the control of plant development, lessons from shoot branching. *The Plant Journal* doi: 10.1111/tpj.12488.

Wang R, Liu S, Wang J, Dong Q, Xu L, Rui Q. 2013. Purification, characterization and identification of a senescence related serine protease in dark-induced senescent wheat leaves. *Phytochemistry* **95,** 118–126.

Watanabe M, Tanaka H, Watanabe D, Machida C, Machida Y. 2004. The ACR4 receptor-like kinase is required for surface formation of epidermis-related tissues in Arabidopsis thaliana *The Plant Journal*. **39,** 298–308.

Winter D, Vinegar B, Nahal H, Ammar R, Wilson GV, Provart N. 2007. An "Electronic Fluorescent Pictograph" browser for exploring and analyzing large-scale biological data sets. *PLoS ONE* **e718,** 10.1371.

Wise AA, Liu Z, Binns AN. 2006. Three methods for the introduction of foreign DNA into Agrobacterium. In: Wang K, ed. *Agrobacterium protocols*, Ed 2, Totowa, NJ, USA: Humana Press Inc., pp. 43–54.

Woo HR, Chung KM, Park JH, Oh SA, Ahn T, Hong SH, Nam HG. 2001. ORE9, an F-box protein that regulates leaf senescence in Arabidopsis. *The Plant Cell* **13,** 1779–1790.

Yang P, Smalle J, Lee S, Yan N, Emborg TJ, Vierstra RD. 2007. Ubiquitin C-terminal hydrolases 1 and 2 affect shoot architecture in *Arabidopsis. The Plant Journal* **51,** 441–457.

Yan H, Saika H, Maekawa M, Takamure I, Tsutsumi N, Kyozuka J, Nakazono M. 2007. Rice tillering dwarf mutant dwarf3 has increased leaf longevity during darkness-induced senescence or hydrogen peroxide-induced cell death. *Genes and Genetic Systems* **82,** 361–366.

Zhang L, Tan Q, Lee R, Trethewy A, Lee YH, Tegeder M. 2010. Altered xylem-phloem transfer of amino acids affects metabolism and leads to increased seed yield and oil content in Arabidopsis. *The Plant Cell* **22,** 3603–3620.

Zhang P, Battchikova N, Jansen T, Appel J, Ogawa T, Aro EM. 2004. Expression and functional roles of the two distinct NDH-1 complexes and the carbon acquisition complex NdhD3/NdhF3/CupA/Sll1735 in Synechocystis sp PCC 6803. *The Plant Cell* **16,** 3326–3340.

Zhu H, Kranz RG. 2012. A nitrogen-regulated glutamine amidotransferase (GAT1_2.1) represses shoot branching in Arabidopsis. *Plant Physiology* **160,** 1770–1780.